

BUREAU INTERNATIONAL DES POIDS ET MESURES



A Study of $^{127}\text{I}_2$ Cells

Using Laser Induced Fluorescence Techniques

by Susanne Fredin-Picard

PAVILLON DE BRETEUIL
F-92312 Sèvres Cedex
France

Bureau International des Poids et Mesures

Rapport BIPM 89/5

A Study of $^{127}\text{I}_2$ Cells
Using Laser Induced Fluorescence Techniques

by Susanne Fredin-Picard

Abstract

An experimental method has been tested to compare impurity levels in iodine cells used in the saturated absorption of lasers. The method is based on the use of the Stern-Volmer formula where the laser induced fluorescence of iodine is studied as a function of pressure.

Measurements of a number of iodine cells are included as a demonstration and test of this experimental method. The frequency shift has been measured for each cell using saturated beat frequency absorption and has been connected indirectly to the Stern-Volmer formula. It is found that the method is relevant for cells with low to moderate concentration of impurities.

Table of Contents

1 Introduction	5
2 Theoretical Considerations	7
2.1 The Relaxation Processes	7
2.2 The Stern-Volmer Formula	8
2.3 Calculation of the Pressure	11
2.4 The Normalized Stern-Volmer Formula	12
2.5 Additional Phenomena	14
3 Experimental Procedure	15
3.1 The Excitation Process	15
3.2 Experimental Arrangement	17
3.2.1 The Excitation Apparatus	17
3.2.2 The Iodine Cell	19
3.2.3 The Detection System	22
3.3 Numerical Treatment	24
4 Results and Analysis	24
4.1 Preliminary Results on I27I2	24
4.1.1 The Stern-Volmer Curve	24
4.1.2 Reproducibility	26
4.2 Comparison of Iodine Cells	27
4.2.1 Stern-Volmer Slope and Frequency Shift of Some Cells	27
4.2.2 Cross Sections	32
4.2.3 An Attempt at a Quantitative Analysis	32
4.2.4 Impurity Concentration and Frequency Shift Correlation	34
4.3 I29I2	36
4.4 Discussion	36
4.4.1 Influencing Factors	36
4.4.2 Future Aspects	37
5 Conclusion	38
6 References	39

1 Introduction

Doppler-free spectroscopy techniques are nowadays used with the aim of isolating individual hyperfine components to which a laser frequency can be locked. Molecular iodine has been shown to be very useful in the development of laser frequency stabilization. It has a rich of spectrum in the visible, which allows coincidences between laser lines and molecular transitions to be found without too much difficulty. As a matter of fact, four of the five radiations used for the practical realization of the definition of the metre, recommended by the 17th CGPM¹ 1983 [1], belong to iodine.

Iodine vapor can be kept in a glass cell. In practice, an iodine cell does not always remain the same. Due to degassing from the glass walls, the concentration of unwanted impurities generally increase with time [2], especially for cells which are originally strongly polluted². The impurities can come from the glass walls of the cell, the iodine itself and the handling when the glass cell is filled with iodine vapor.

It has been shown that the frequencies of the hyperfine components of a molecule are shifted by the presence of foreign atoms or molecules [4]. In metrology our aim is to measure the magnitude of this frequency shift and, if possible, to remove it. The former has already been done successfully by using the method of saturated absorption beat frequency [5]. This means that the beat frequency between two laser saturated hyperfine components of a gas is studied; one component being saturated by the laser system of interest, the other component saturated by a reference laser system. By detecting the third derivative of each hyperfine line, the lasers can be frequency stabilized and hence provide a frequency standard. This method offers a very good relative frequency determination which at the moment has reached a relative uncertainty of 1 part in 10^{11} , see for example [6,7,8,9,10].

Although the saturated absorption beat frequency technique is a precise method, the experimental procedure is time consuming. It involves installing the iodine glass cell into an internal cavity laser system, and time waiting for the system to become mechanically and thermally stable. It would therefore be more convenient to use an alternative and complementary experimental test method that is possibly more flexible and takes less time.

There exist several possibilities for the measurement of the concentration of impurities of an iodine glass cell in addition to the method mentioned above. One method has successfully been realized using the Hanle effect, in which the polarisation of the fluorescence from iodine is studied when applying an external magnetic field [11]. One can in this way indirectly measure the lifetime, which is pressure dependent and is effected by the presence of foreign gases. Another way is to measure directly

¹ Conférence générale des poids et mesures

² It should be pointed out that Rowley et al. [3] on the contrary have not observed any degradation with time in their iodine cells.

the lifetime of the level being studied [12,13]. Yet, another method that has been attempted is to study the connection between frequency shifts of the hyperfine components and the spectral characteristics of the impurities [14].

We have chosen to use a fifth method. Experimentally it requires that the intensity of the laser induced fluorescence be studied as a function of the iodine pressure. The intensity of the fluorescence at a certain pressure is dependent on the concentration of impurities; the more impurities there are, the higher is the probability of collisional quenching³. The probability of collisional quenching is high when the excited level has a long life time. The relation between intensity of fluorescence and iodine pressure can be described by the Stern-Volmer formula [15].

This method offers several advantages:

- 1) It does not demand a high mechanical stability of the laser and associated optics.
- 2) One can use a laser working in multimode.
- 3) The size of the cell being studied is not restricted
- and 4) The experimental setup is comparatively compact and modest.

Spieweck has successfully tested the Stern-Volmer formula on 23 iodine cells [16]. It is therefore of interest for the BIPM to further study this method, in order to obtain an easy way to test iodine cells, and to compare it with the saturated absorption beat frequency method which we have used previously. We further intend to use these two complementary methods in a larger systematic international inter comparison of iodine cells in the near future.

We will in the next section give a review of the theory behind this experiment. The experimental procedure is described in Sec. 3. The results will be shown and discussed in Sec. 4.

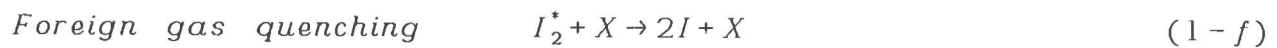
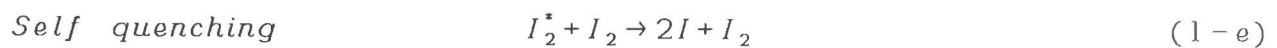
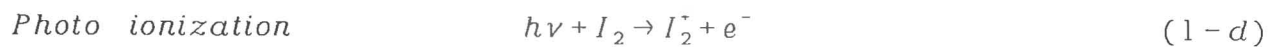
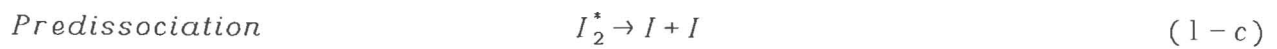
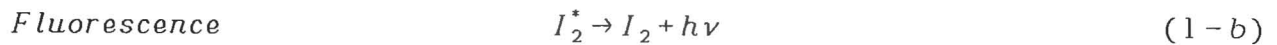
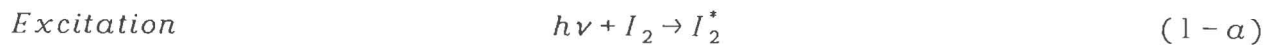
³ We mean here an induced relaxation process caused by collision without giving rise to any emission.

2 Theoretical Considerations

We will in this section review the theory which describes the relationship between the iodine pressure and the fluorescence. Some associated phenomena will also be discussed.

2.1 The Relaxation Processes

In addition to the transition oscillator strength and Franck-Condon and Hönl-London factors, the intensity of fluorescence of a particular transition depends on other competing relaxation processes, such as ionization, predissociation and collisional quenching. The main processes involved in our case can be represented as



where $h\nu$ represents a photon, X a foreign gas molecule (or atom), e^- represents an electron and the + indicates that the iodine molecule is ionized. Here and elsewhere the symbol * indicates that the molecule is excited.

The ionization potential (I.P. = 9.311 eV [17]⁴) is much higher than the energy region being excited (around 3.3 eV), and the exciting light is not intense enough to produce a multiphoton process. We therefore completely disregard ionization and concentrate on the three processes (1-c), (1-e) and (1-f) mentioned above.

2.2 The Stern-Volmer Formula

The main processes that contribute to the observed lifetime of a state are radiative, non-radiative and collision induced (quenching) processes. The first two processes concern mainly spontaneous emission and predissociation. The total effective lifetime τ_{eff} can then be expressed as

$$\frac{1}{\tau_{\text{eff}}} = \frac{1}{\tau_r} + \frac{1}{\tau_{nr}} + \frac{1}{\tau_c} \quad (2)$$

where τ_r , τ_{nr} and τ_c are the contributions mentioned above respectively.

The basic expression describing exponential decay from a state with the lifetime τ can be written as

$$N = N_0 e^{-t/\tau} \quad (3)$$

where N is the number of populated sites of the state at the time t and where N_0 is the number of populated sites at the time t=0. With this formula in mind we can easily construct a model which describes the influence of the spontaneous emission, predissociation and collisional quenching of the population of the excited state. We hence write

$$\frac{d[I_2^*]}{dt} = -\frac{[I_2^*]}{\tau_r} - \frac{[I_2^*]}{\tau_{nr}} - S[I_2^*][I_2] - Q[I_2^*][X] \quad (4)$$

⁴ We use the unit of eV due to its convenience in spectroscopic work.

where $[I_2^*]$, $[I_2]$ and $[X]$ are the concentration of excited iodine molecules, iodine molecules in the ground state and foreign gas atoms-molecules respectively. S and Q represent the collision rate of excited iodine molecules with ground state iodine and foreign molecules respectively.

When saturation is avoided, there should exist an equilibrium between the excitation rate and the decay rate, that is to say

$$\frac{d[I_2^*]}{dt} = -\sigma_A I_0 [I_2] \quad (5)$$

where I_0 is the irradiance (i.e. number of photons per area and time), and where σ_A is the absorption cross section⁵. If we let σ_S and σ_X represent the cross section of the self collisions and collisions between foreign gases and iodine, one can define S and Q as [18,19]

$$S = v_I \sigma_S \quad (6-a)$$

$$Q = v_X \sigma_X \quad (6-b)$$

v_I and v_X are the mean velocity of iodine and foreign gas molecules respectively. The mean velocity v as given by Maxwell-Boltzmann statistics can be expressed as

$$v = \sqrt{\frac{8}{\pi} \frac{kT}{\mu}} \quad (7)$$

k is here the Boltzmann constant and μ indicates the reduced mass between the colliding particles. This means that S and Q can be written as

$$S = \sigma_S \sqrt{\frac{16}{\pi} \frac{kT}{M_I}} \quad (8-a)$$

$$Q = \sigma_X \sqrt{\frac{8}{\pi} \frac{kT}{\mu_X}} \quad (8-b)$$

where M_I is the mass of the iodine molecule and μ_X is the reduced mass of the iodine and the foreign gas molecule.

⁵ Note that the meaning of σ varies. Here we define "cross section" as the squared collision diameter times π .

Using the equations (4), (5), (8-a) and (8-b) we obtain the following formula⁶.

$$\sigma_A I_0 [I_2] = [I_2^*] \left(\frac{1}{\tau} \right) + \sigma_S v_I [I_2^*] [I_2] + \sigma_X v_X [I_2^*] [X] \quad (9-a)$$

where τ is given by

$$\frac{1}{\tau} = \frac{1}{\tau_r} + \frac{1}{\tau_{nr}} \quad (9-b)$$

We now connect the intensity of the fluorescence I_F (number of photons per area and time unit) caused by spontaneous emission with the population of the excited state:

$$I_F = A [I_2^*] \quad (10)$$

A is the transition probability, which is related to the Einstein coefficients (see for example Sakurai et al. [21]). Performing this substitution into Eq. (9-a) we obtain

$$\frac{1}{I_F} = \frac{1}{\sigma_A I_0 A} \left(\frac{1}{[I_2]} \left(\frac{1}{\tau} + \sigma_X v_X [X] \right) + \sigma_S v_I \right) \quad (11)$$

However, this formula is not very useful as the number of molecules is not directly measurable. If we instead use the ideal gas law as an approximation in order to find the pressure that corresponds to the number of molecules we obtain

$$[I_2] = \frac{p_I}{kT} \quad (12)$$

where p_I is the iodine pressure in Pa. Combining Eqs (11) and (12) results in the following expression:

$$\frac{1}{I_F} = \frac{1}{\sigma_A I_0 A} \left(\frac{1}{p_I} \left(\frac{1}{\tau} + \sigma_X v_X \frac{p_X}{kT} \right) kT + \sigma_S v_I \right) \quad (13)$$

in where p_X is the foreign gas pressure. We can here note that the product $\sigma_X v_X p_X / kT$ represents the inverse of the collisional quenching lifetime τ_c . This seems logic; the more molecules there are (higher p_X) or the higher the cross section is,

⁶ This is identical with Eq. (4) of [20], but where a v_2 is missing in the last term.

the less time it will take for the iodine molecule to experience a collision.

If only a small part of the iodine cell is cooled (the "cold finger") under the condition that the iodine is saturated, the cold finger temperature will only influence the gas pressure of the iodine. We can then rewrite Eq. (13) as a linear equation:

$$\frac{1}{I_F} = K \frac{1}{P_I} + L \quad (14-a)$$

where

$$K = \left(\frac{1}{\tau} + \sigma_x v_x \frac{P_x}{kT} \right) \frac{kT}{\sigma_A I_0 A} \quad (14-b)$$

and

$$L = \frac{\sigma_s v_I}{\sigma_A I_0 A} \quad (14-c)$$

The formula given by Eq. (14-a) is often known as the Stern-Volmer formula [15]. K carries the pressure of foreign gas. Observe here that a state with a longer lifetime provides a higher sensitivity in K to p_x than with a short lifetime. K will be bigger for a polluted cell than for a clean one. This enables us to compare iodine cells without knowing the cross sections involved only by comparing K ; all we have to know is the temperature and the relative intensity of the fluorescence.

2.3 Calculation of the Pressure

A convenient way to alter the pressure is to cool a small part of the iodine cell where the saturated iodine is trapped. There exist several empirical and analytical equations for the vapor pressure/temperature relation for iodine of which the derivation of some is discussed by Nesmeyanov [22]. We have chosen to use the transformation formula, Eq. (15), presented by Gillespie and Fraser [23], which is sufficiently accurate for our use in the pressure region being studied⁷.

$$\log p = -\frac{3512.830}{T} - 2.012 \log T + 13.374 \quad (15)$$

⁷ An improved expression of the solid heat capacity of iodine has previously been presented by Lindenberg [24].

where T is given in K and p is the vapor pressure of the solid iodine in atmospheres.

2.4 The Normalized Stern-Volmer Formula

As it is difficult to measure the intensity of the fluorescence in absolute values conserving the experimental conditions, it is convenient to normalize the Stern-Volmer equation. Therefore, the intensity was measured in arbitrary units for each temperature. A computer program transformed temperature into pressure using Eq. (15). The program fitted all the experimental points into a straight line using the right mean square method. The normalization of intensity is done by dividing Eq. (13) by I_0 where I_0 is the recalculated intensity at 10 Pa (9°C) using Eq. (14). This means that

$$0.1 K_0 + L_0 = 1 \quad (16)$$

where K_0 and L_0 are the normalized parameters. This gives us

$$\frac{I_0}{I_F} = \frac{\sigma_S v_I + \frac{1}{p_I} \left(\frac{kT}{\tau} + \sigma_X v_X p_X \right)}{\sigma_S v_I + \frac{1}{10} \left(\frac{kT}{\tau} + \sigma_X v_X p_X \right)} \quad (17 - a)$$

which also can be written on the form

$$\frac{I_0}{I_F} = K_0 \frac{1}{P_I} + L_0 \quad (17-b)$$

from which K_0 and L_0 explicitly can be obtained, that is,

$$K_0 = \frac{\frac{kT}{r} + \sigma_X v_X P_X}{\sigma_S v_I + \frac{1}{10} \left(\frac{kT}{r} + \sigma_X v_X P_X \right)} \quad (18)$$

and

$$L_0 = \frac{\sigma_S v_I}{\sigma_S v_I + \frac{1}{10} \left(\frac{kT}{r} + \sigma_X v_X P_X \right)} \quad (19)$$

The standard deviation ΔK_0 in K_0 is obtained as [25]

$$\Delta K_0 = \sqrt{\frac{1 \sum_{i=1}^n (I_{calc_i}^{-1} - I_{obs_i}^{-1})^2}{\sum_{i=1}^n (p_{i^{-1}} - \overline{p_{i^{-1}}})^2 (n-2)}} \quad (20)$$

where $\overline{p_{i^{-1}}}$ is the mean value of the inverse pressure of n data points. I^{-1} is the normalized inverse intensity of the fluorescence (see Eq. (17)), and i indicates the i^{th} data point.

2.5 Additional Phenomena

It is worth mentioning some additional phenomena which can influence the measurements. For example, quenching can also be caused by collisions with the cavity walls. We disregard this effect, referring to previous works (see for example Capelle and Broida [18] with references).

Another unwanted process is the radiation trapping by ground state molecules. Ornstein and Derr [20] have studied this aspect. They preferred to base their calculations of self quenching cross sections using iodine pressures lower than 0.12 torr (lower than 16 Pa) for this reason. We have not seen any direct evidence for radiation trapping, see also section 4.4.1.

A third possible phenomenon is the transfer caused by collisions to other radiative ro-vibrational states within the same electronic state [2,26,27,18]. We estimate this effect to be of second order, though no further investigation has been done yet on this subject from our behalf. It is therefore not included in the development given above.

Finally, considering the linear absorption described by Beer's law, the intensity of the excitation beam is attenuated the further it progresses in the iodine vapor. This implies that the intensity of the fluorescence will be a function of pressure and location in the vapor. It is thus important to choose the observation region close to the side of the cell where the laser beam enters. See also section 4.4.1.

3 Experimental Procedure

3.1 The Excitation Process

The principle of laser induced fluorescence (LIF) is shown in Figure 1-a. One selected energy level is excited, which relaxes through fluorescence to lower energetically levels according to the selection rules. The exciting wavelength might accidentally be coincident with several transitions due to its line width.

We have chosen the exciting wavelength (λ) to be 501.7 nm, although this line is 10 times less intense than 514.5 nm, due the long lifetime of the level being excited [13]. It gives a higher sensitivity for collisional quenching.

Relative intensities in absorption and wavenumbers for the B-X system have been obtained by Luc and Gesternkorn [29] using Fourier transform spectroscopy. The Doppler width at full width half maximum (FWHM) of iodine at room temperature is 500 MHz. The laser line at FWHM is estimated to be 5 GHz after having checked the number of single modes within a profile using a Fabry-Perot interferometer. This implies that five iodine rotational lines can be excited using $\lambda=501.71$ nm [28], namely the R(49) 67-0, R(39) 64-0, R(26) 62-0, R(54) 70-0 and the R(55) 71-0 lines. The R(26) 62-0 line gives the main contribution to the observed fluorescence [30,31] whose upper energy level is furthest away from the dissociation limit of the five lines mentioned above.

The excitation process involved in the experiment described above is schematically represented in Fig.1-b. The $J'=27$ $v'=62$ level of the $B^3\Pi_{0_u}^+$ state is excited from the ground state $X^1\Sigma_g^+$. Only the lowest vibrational levels of the ground state are populated. The change in the rotational quantum number obey the selection rule $\Delta J=\pm 1$. This results in two possible ways to relax into a lower state; either through a P-line ($\Delta J=-1$) or through an R-line ($\Delta J=+1$). The strongest transitions are the ones favoured by the Franck-Condon factors.

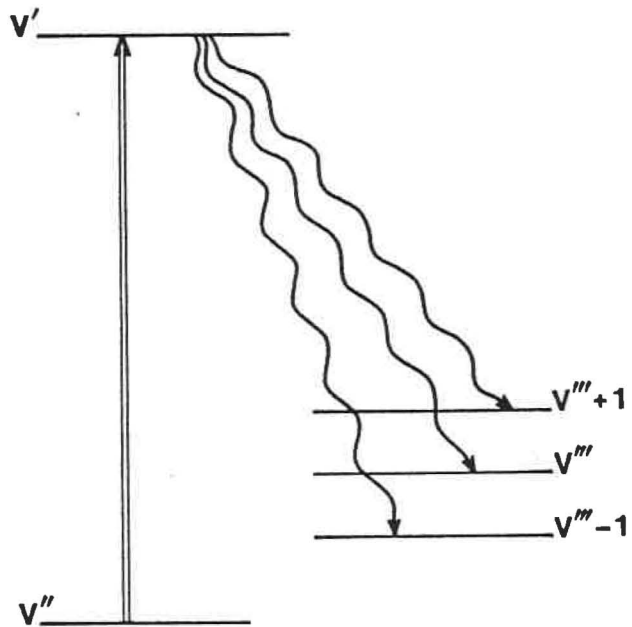


Fig.1-a. Schematic principle of LIF. By excitation of a selected ro-vibronic level of a certain electric state, fluorescence can be observed. It corresponds to transitions, allowed by the appropriate selection rules, to lower energy levels.

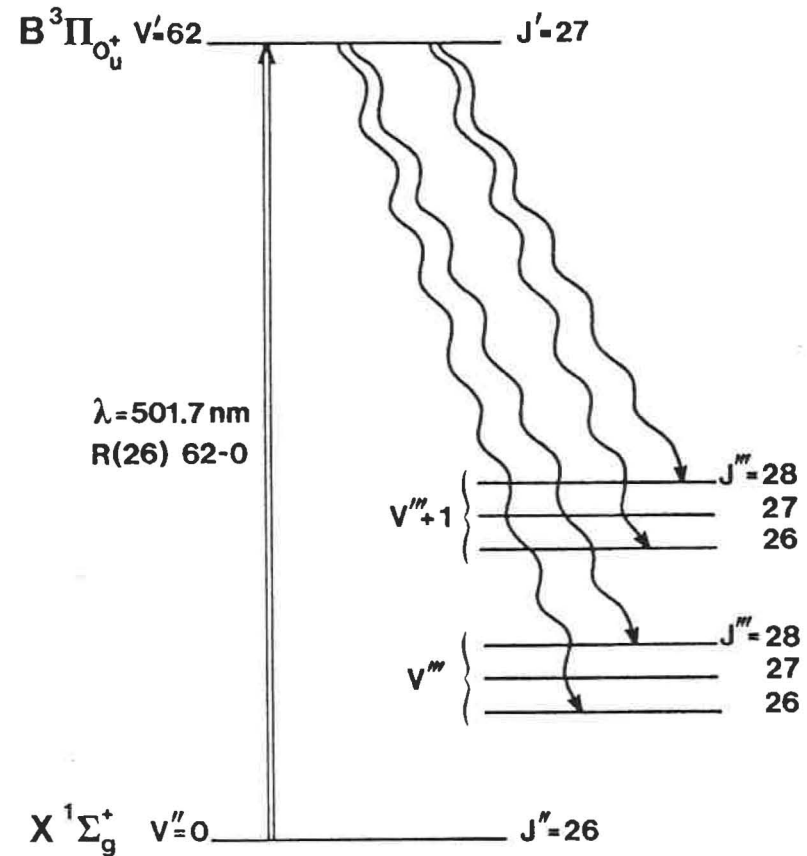


Fig.1-b. Transition scheme corresponding to excitation of $J'=27, v'=62$. The fluorescence will here correspond to transitions from the B state into lower vibrational levels v''' of the X state, where J'' is either 28 (giving a P-line) or 26 (giving a R-line).

3.2 Experimental Arrangement

The experimental arrangement is shown schematically in Fig.2. We divide the experimental arrangement into three parts: 3.2.1) the excitation apparatus, 3.2.2) the iodine cell and 3.2.3) the detection system. Most of it was contained in a black painted box, where each part mentioned above was separated by a black wall, with holes where the laser beam and the fluorescence radiation could pass.

3.2.1 The Excitation Apparatus

The iodine contained in a glass cell was excited by an argon ion laser (Lexel 95) working in multi mode. The intensity of the laser beam was kept rather low in order to avoid effects of broadening of the laser line [31]. The beam was chopped mechanically (Ealing 28-7615) at between 300 and 400 Hz, and expanded by a lens system. It was further attenuated to an intensity around 20 mW/cm² using neutral density filters (Oriel) so that saturation effects were avoided [32]. A diaphragme was introduced to avoid as far as possible the background fluorescence originating from the laser itself and to choose the diameter of the laserbeam. The optical arrangement belonging to this part is shown in Fig. 3. The laser beam was up to 98% linearly polarized.

The laser beam was directed through the optics by a mirror periscope. All optics (Spindler & Hoyer) were rigidly mounted on an optical bench (Microcontrolle). Most other mechanics were constructed at the work shop of the BIPM. The intensity stability of the laser was monitored by letting a small part of the beam being detected by a commercial power meter (Lexel model 504) and registering the power meter output simultaneously with the recorded fluorescence.

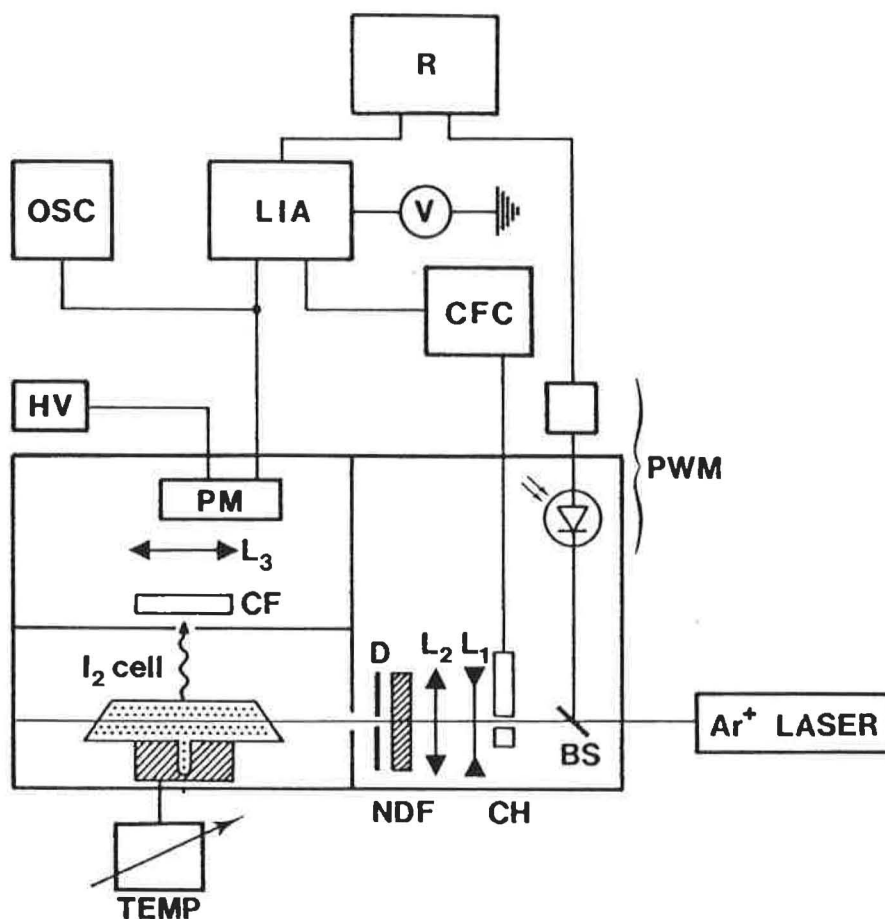


Fig.2. Schematical representation of the experimental setup used for the Stern-Volmer measurements. Ar^+ laser light at 501.7 nm was chopped, beam expanded by a lens system (L_1 and L_2) and set at an intensity of about 20 mW/cm^2 by neutral density filters (NDF) in order to excite a selected ro-vibronic level of the B state in iodine. A diaphragm (D) was used to control the beam diameter. The iodine pressure was varied and controlled by a Peltier battery cooled servo controlled cold finger (TEMP). The fluorescence, marked in the figure by a wavy arrow, was focused onto a photomultiplier (PM) by a lens (L_3). The photo multiplier worked between 500 and 700 V taken from a high voltage (HV) supplier. Most of the diffused laser background light was cut off by a colour filter (CF). The signal coming directly from the photomultiplier could be seen on an oscilloscope (OSC). The signal was further amplified by a lock-in amplifier (LIA). A chopper frequency control (CFC) provided a frequency at 300-400 Hz to the chopper (CH). This signal was used as a reference to the lock-in amplifier. The output signal from the latter was controlled by a volt meter (V) and displayed graphically on a recorder (R). A small part of the incoming laser beam was linked off by a beam-splitter (BS) onto a power meter (PWL) and traced simultaneously on the recorder.

3.2.2 The Iodine Cell

Most of the iodine cells used at the BIPM are made of fused silica with a pyrex transition. They have all been filled with iodine at the BIPM since 1972 [33], of which a great number of cells contain very low fractions of impurities and hence show small frequency shifts.

The iodine pressure in the cell was set by the "cold finger" method, where the saturated iodine is trapped in a cooled part of the cell. The rest of the cell was kept at room temperature. The cooling was obtained by two series-coupled Peltier elements. To ensure a good thermal contact a silicon thermal paste was used. The temperature calibration was estimated to deviate by not more than 0.1 °C. With the aide of a servo system, the temperature was stable within a minute, which meant a temperature variation of about 0.02°C. The glass cell itself was put on a support which height and inclination could be adjusted, and is shown in Fig. 4-a (where also a photo multiplier is seen from behind, see below).

The fluorescence was allowed to leak out through a hole. Using a hole of 1 cm in diameter, most molecules should be relaxed before leaving the observation region, taking account of the lifetime of the excited level (14 μ s) [13] and the mean thermal velocity of the iodine molecules (156 m/s, see Eq. (7) above).

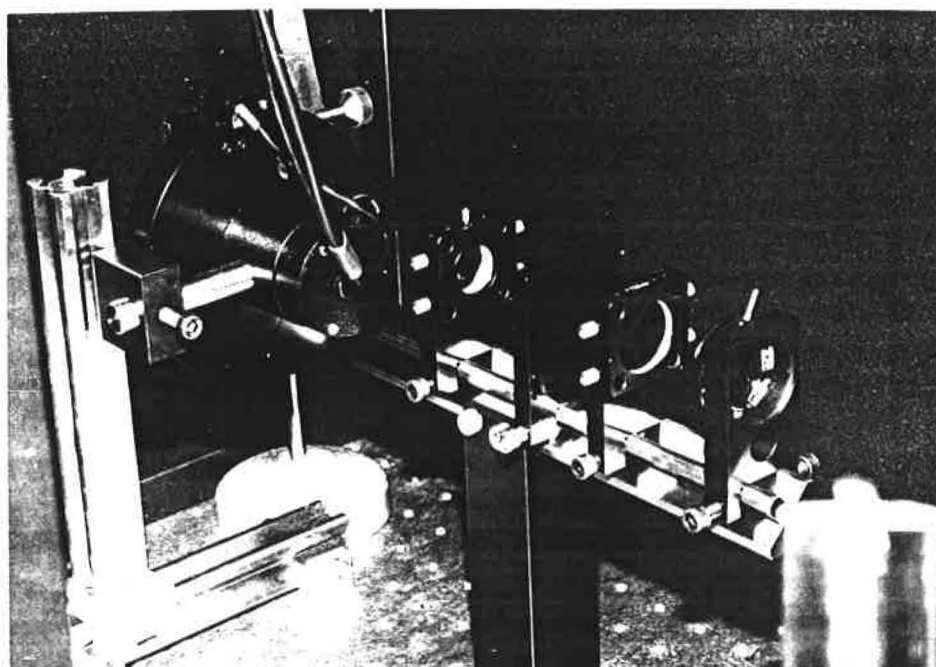


Fig.3. Optical arrangement where the chopper, the lens system and the filter holder are seen.

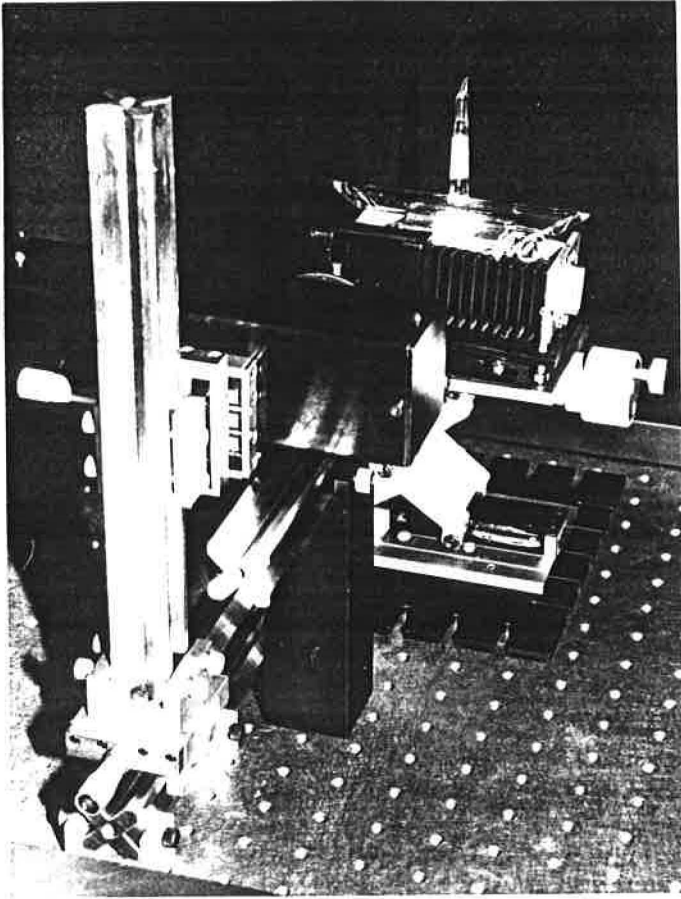


Fig.4-a. Iodine cell on its adjustable support and the photomultiplier seen from behind.

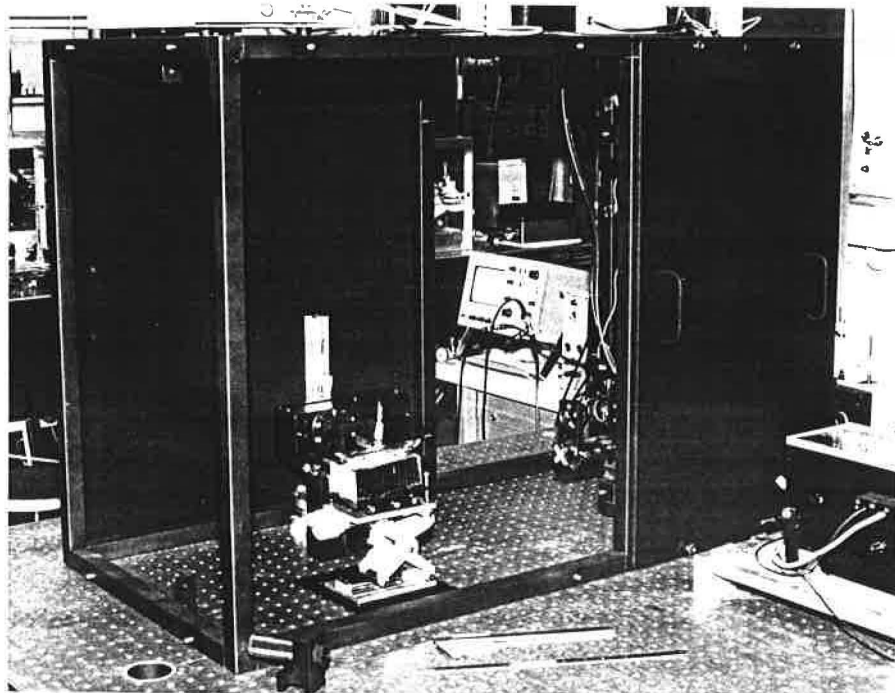
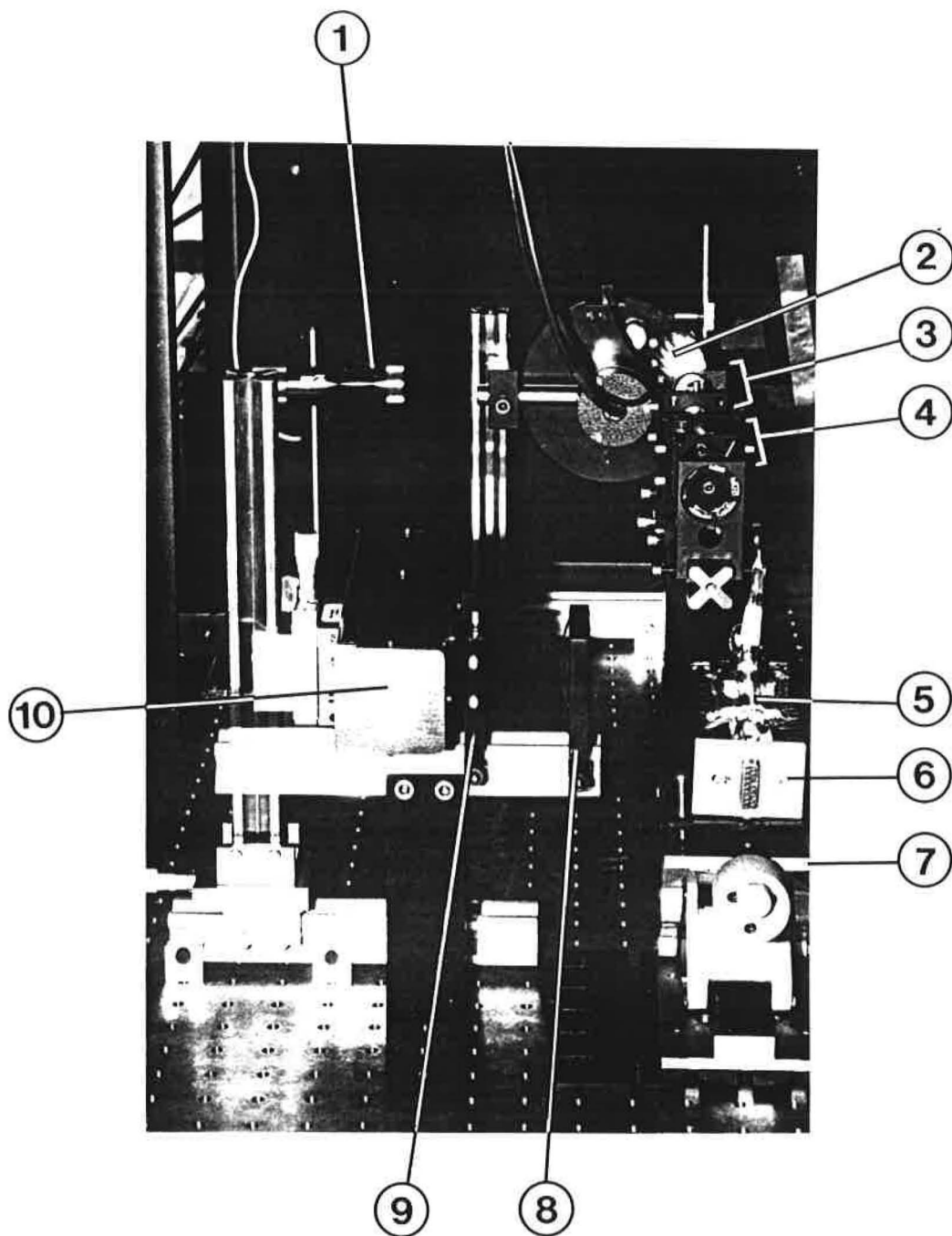


Fig.4-b. Photomultiplier and iodine cell. The photo multiplier is put into a black box in order to simplify the mechanical mount and electric connections.



- ① Laser power meter PWM
- ② Chopper (CH)
- ③ Beam expanding system (L_1 and L_2)
- ④ Neutral density filter and diaphragm (NDF and D)
- ⑤ Iodine cell
- ⑥ Peltier cooling element
- ⑦ Adjustable support
- ⑧ Colour filter
- ⑨ Lens (L_3)
- ⑩ Blinded photomultiplier

Fig.5. The whole experimental setup where the dividing walls have been taken away temporarily.

3.2.3 The Detection System

During a scan the fluorescence light focused onto a photo multiplier (Hamamatsu R955) was recorded while the temperature of the Peltier batteries was varied. The photo multiplier was connected to a high voltage power supply (EG&G Ortec 556H). The dark current was 9-10 nA. Most of the scattered laser light was absorbed before it could reach the photomultiplier by a colour filter (Schott OG550). The cell and the photomultiplier with the black container open is shown in Fig. 4-b. The whole experimental setup is shown in Fig.5 where the dividing walls have been removed.

The signal from the photomultiplier was observed on an oscilloscope, passed to a phase sensitive detector and amplified by a lock-in amplifier (Brookdeal 401A), where the chopper frequency was used as reference signal. The oscilloscope signal is shown in Fig. 6. The signal amplitude was 150 mV at 700 V on the photo multiplier using a chopper frequency of 300 Hz.

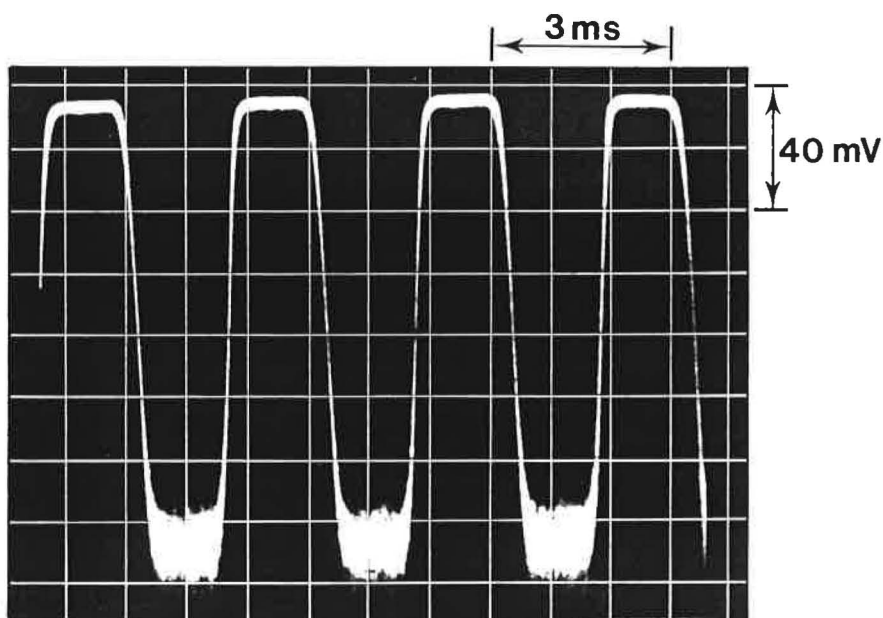


Fig.6. Photo multiplier signal seen on the oscilloscope. The bias voltage was about 700 V.

It was important to regularly control the zero level, due to the drift in the lock-in amplifier zero level. The amplified signal was observed on a volt meter and recorded by a chart recorder simultaneously with the detected laser intensity. The fluorescence intensity was corrected for drift in laser power.

An example of the detected signal during a measurement is shown in Fig. 7. A 5 cm long iodine cell named BIPM52 was used here. The intensity of the fluorescence is shown as a function of time and temperature. The laser intensity is shown in the top of the figure.

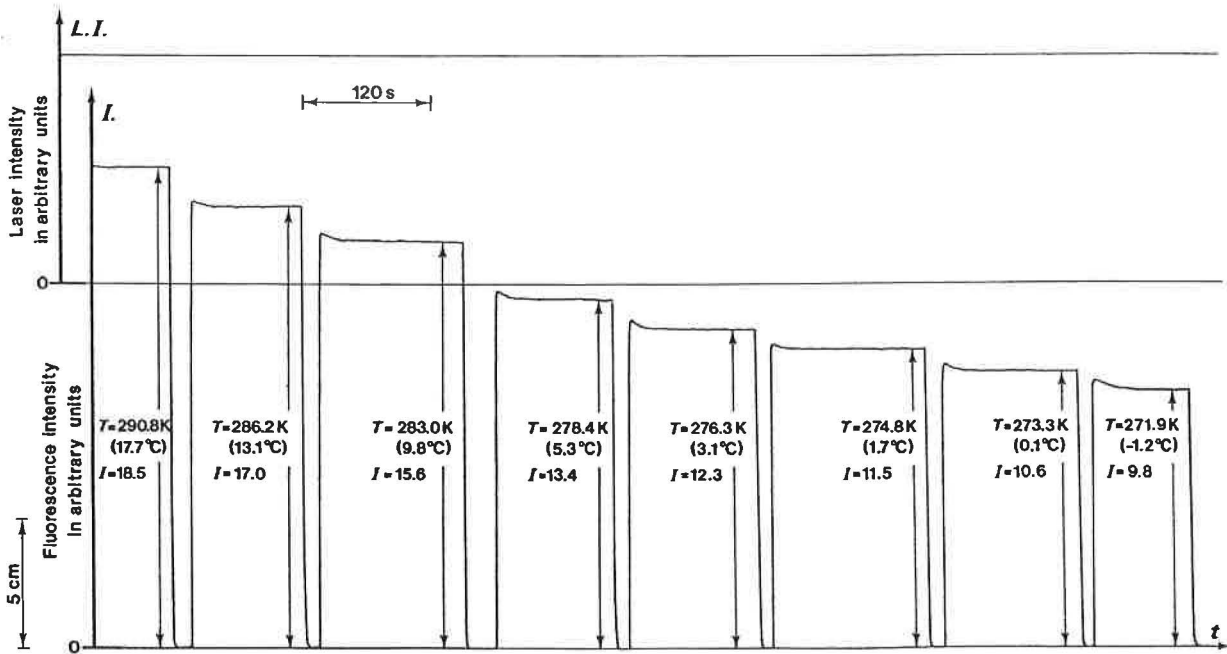


Fig.7. Raw data obtained on the recorder. The time (t) is indicated in the very bottom of the diagram. The laser intensity (L.I.) is in the top. The intensity (I) of the fluorescence makes a decreasing step each time the temperature (T) is decreased. The intensity "drop" in fluorescence corresponds to a cut laserbeam in order to control the zero level drift of the lock-in amplifier.

3.3 Numerical Treatment

The measured data is treated by a computer program written in Turbo Pascal, where the data is fitted and stored. It can hence easily be presented in a numerical and graphical form.

4 Results and Analysis

We have shown in Sec. 2 that that a knowledge of the slope of the Stern-Volmer curve gives enough information to compare the impurity content in different iodine cells. As a demonstration and test of the current technique we have made a series of measurements on iodine cells. The correlation between the frequency shift for cells used in frequency stabilized laser systems and their impurity concentration is demonstrated.

4.1 Preliminary Results on $^{127}\text{I}_2$

4.1.1 The Stern-Volmer Curve

The data was represented in a diagram where the reciprocal intensity was shown as a function of the reciprocal iodine pressure; the Stern-Volmer curve. An example of a Stern-Volmer curve is shown in Fig. 8, which is the diagram of the experimental data shown in Fig.7. The measured cell showed a frequency shift $\Delta\nu=[21.6 \pm 1.7]$ kHz⁸. The uncertainty bars indicate an uncertainty in temperature of 0.1°C and a relative uncertainty in observed intensity of about $\pm 0.6\%$ at 23 Pa (18°C). The individual uncertainty increases with decreasing pressure and intensity and corresponds to a relative uncertainty in K_0 of at most $\pm 2\%$. The slope K_0 is here $[3.19 \pm 0.02]$ Pa. We can see in Fig. 8 that the a straight line fits well.

⁸ The beat frequency measurements were performed using intra cavity HeNe lasers with $\lambda=633$ nm stabilized on iodine, using the BIPM7 and BIPM2 lasers.

It was soon found that the experimental data were well described by the Stern-Volmer function of Eq. (17). However, it was observed that the data obtained at high pressure for cells with $K_0 < 2$ Pa were not sensitive to temperature. It was verified that this effect did not arise from saturation. The data points for $p_I > 12.5$ Pa for these cells were therefore eliminated in the fitting. It seems however unlikely that this effect should be caused by the radiation trapping proposed by Ornstein and Derr [20], which then ought to be observed also for the worse cells. Maby this observation is an effect of Beer's law, see further section 4.4.1. The bad cells required a longer time to show a stable fluorescence than the good cells when the cell was cooled.

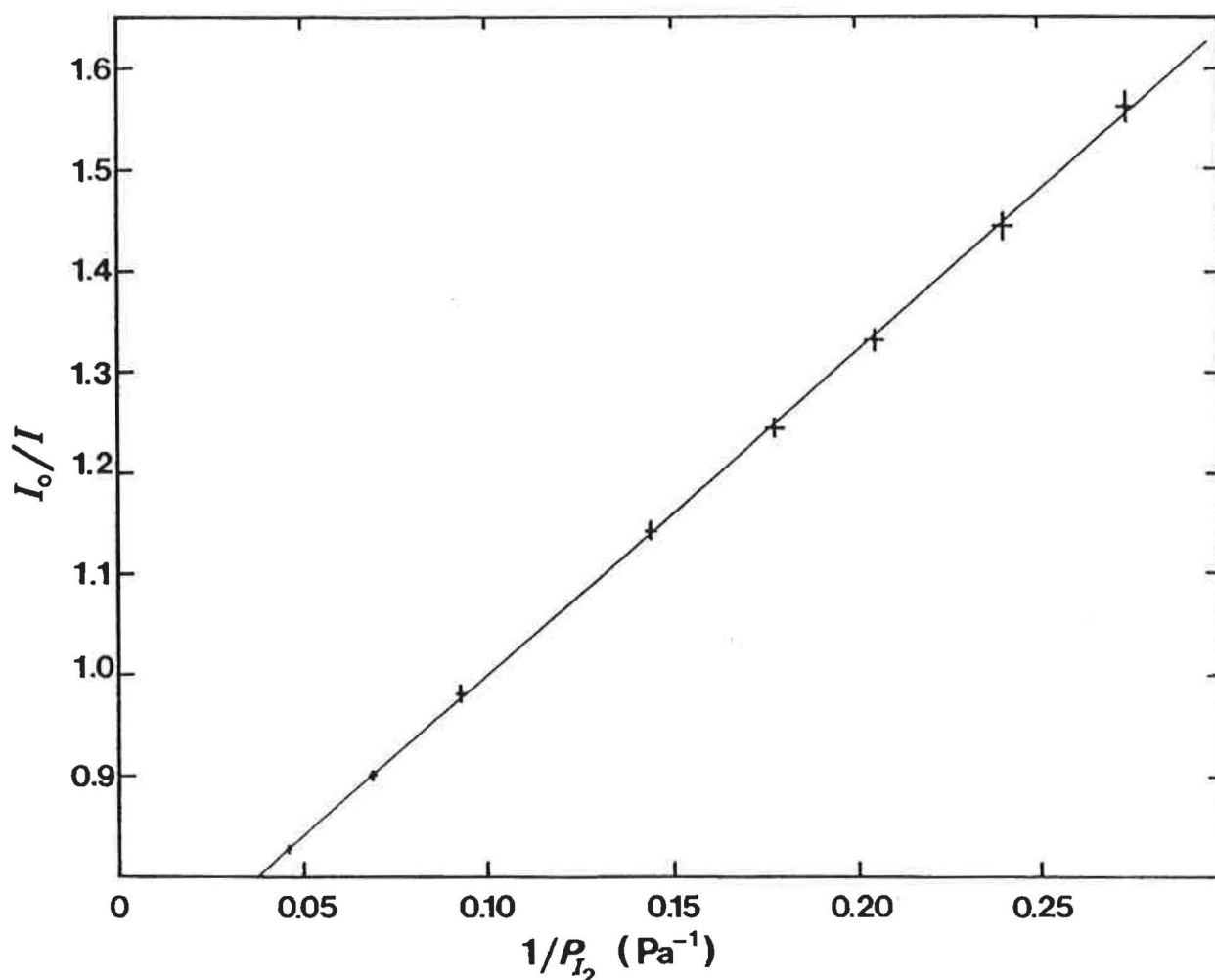


Fig.8. Stern-Volmer diagram using the experimental data displayed in Fig. 7. The normalized reciprocal intensity is shown as a function of the reciprocal iodine pressure in the cell. The uncertainty bars correspond to an uncertainty of 0.1°C and 1 mm intensity registration by the recorder with a 20 cm full signal.

4.1.2 Reproducibility

The reproducibility of the method described above was tested in general by repeating the measurement of the same cell after it had been replaced by another one in between each measurement. The result of this test is shown schematically in Fig. 9-a, where the slope of 30 different measurements of the same cell is shown as a function of each measurement event. The individual errors of K_0 are marked out by the uncertainty bars. The relative uncertainties of K_0 are in the range 0.1-2.0 %. The mean uncertainty is 0.023 Pa. The mean value and standard deviation is here $[3.12 \pm 0.06]$ Pa and are represented by dashed and dotted lines respectively. This indicates a reproducibility with a relative uncertainty of 1.9%.

The reproducibility is also represented in a histogram in Fig. 9-b. Even though the number of measurements is not large (30 measurements), the distribution behaves already like a normal distribution to the extent that 67% of the data are within ± 1 standard deviation.

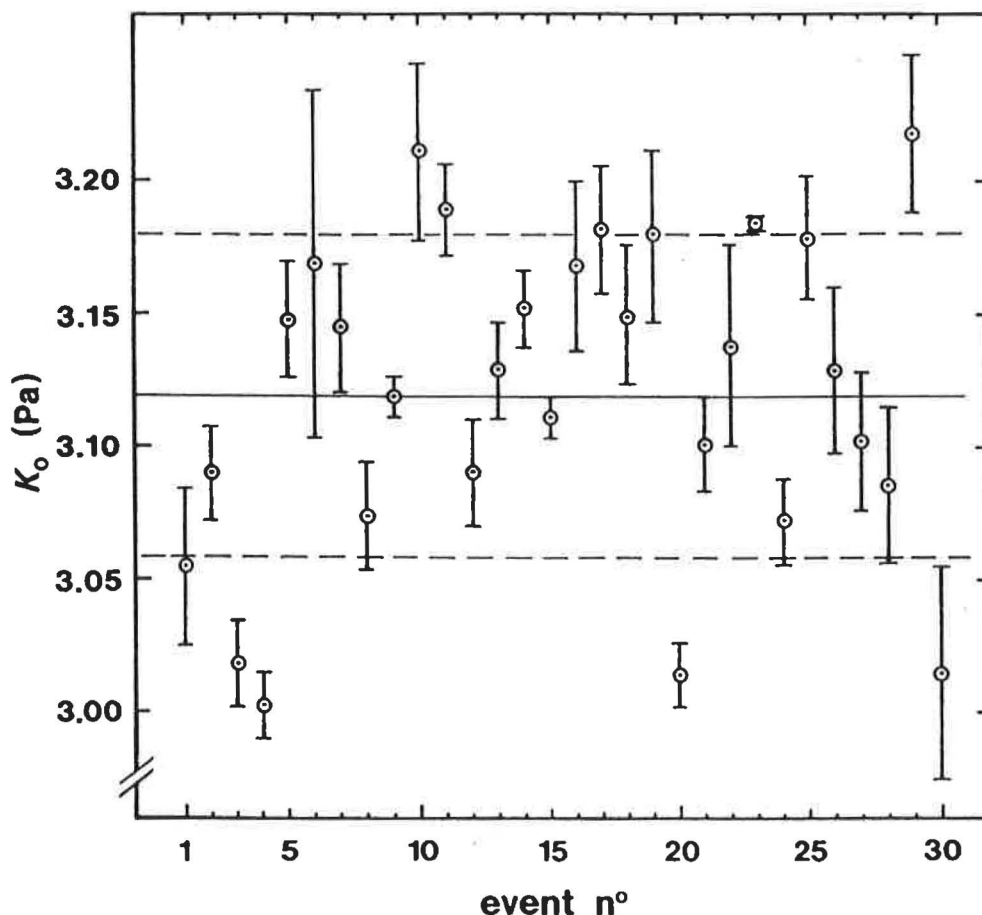


Fig.9-a. Representation of the reproducibility of the Stern-Volmer measurements of the BIPM52 iodine cell. The individual uncertainties in K_0 (the slope of the Stern-Volmer curve) are indicated by the bars. The mean value is marked by a solid line and the standard deviation by a dashed one.

The development of the mean value of K_0 is shown in the diagram of Fig. 9-c, where the standard deviation and the standard deviations of the mean value are marked with thick and thin bars respectively. The mean value attains a rather stable value after 11 measurements, and is within the standard deviation of 30 measurements after 5 measurements. A certain increase of the initial value can be observed; the reason for this is not known.

4.2 Comparison of Iodine Cells

4.2.1 Stern-Volmer Slope and Frequency Shift of Some Cells

The reproducibility of six different iodine cells are represented in Fig. 10-a in a similar way to that of Fig. 9-a. The slopes are $[1.08 \pm 0.03]$ Pa, $[1.99 \pm 0.03]$ Pa, $[3.12 \pm 0.06]$ Pa, $[4.35 \pm 0.10]$ Pa, $[4.97 \pm 0.03]$ Pa and $[6.42 \pm 0.21]$ Pa respectively. The mean values are indicated by solid lines where the standard deviations are indicated by dashed ones. The same six mean values of K_0 are shown in the Stern-Volmer diagram of Fig. 10-b. The measured frequency shift in kHz is indicated for each cell at the right of the slope. The slope corresponding to the standard deviation is indicated by dashed curves. The standard deviation is not marked where it is so small that it is within the width of the curve itself.

K_0 varied from 1.0 to 6.4 Pa corresponding to frequency shifts from 2 to 187 kHz. It was found that the relation between K_0 and the frequency shift is not linear, which is in full agreement with the results of Spieweck [16]. The relation between the measured frequency shift and the Stern-Volmer slopes for the six cells mentioned above is shown in Fig. 11 with the uncertainty bars indicated.

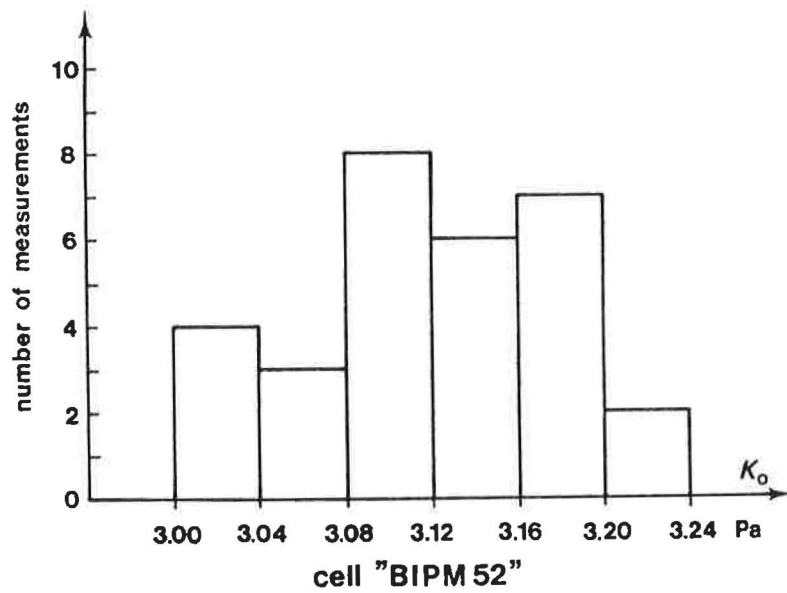


Fig.9-b. Reproducibility for the BIPM52 iodine cell represented in a histogram.

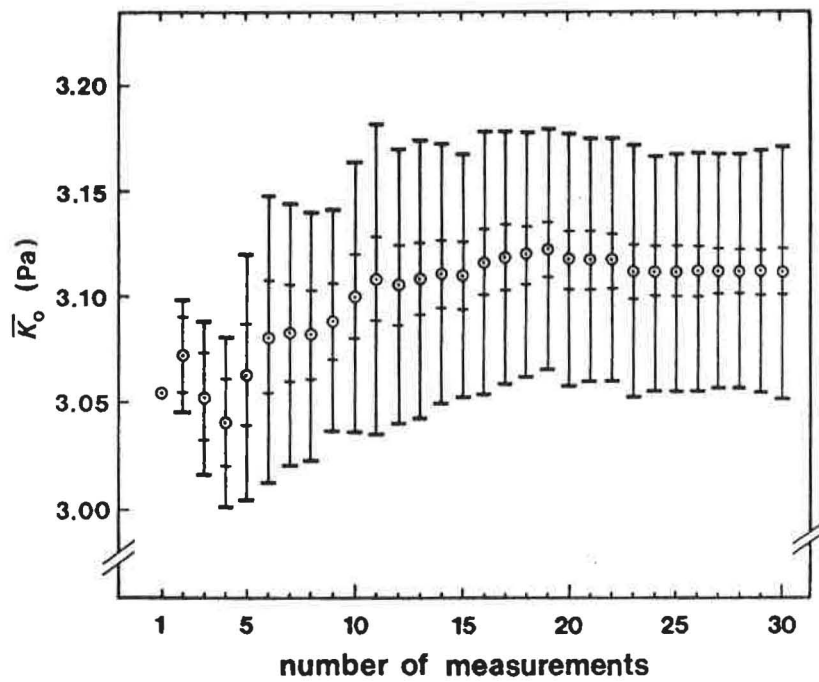


Fig.9-c. Development of the mean value of K_0 after 30 measurements. The standard deviation and the standard deviations of the mean value are indicated by thick and thin uncertainty bars respectively.

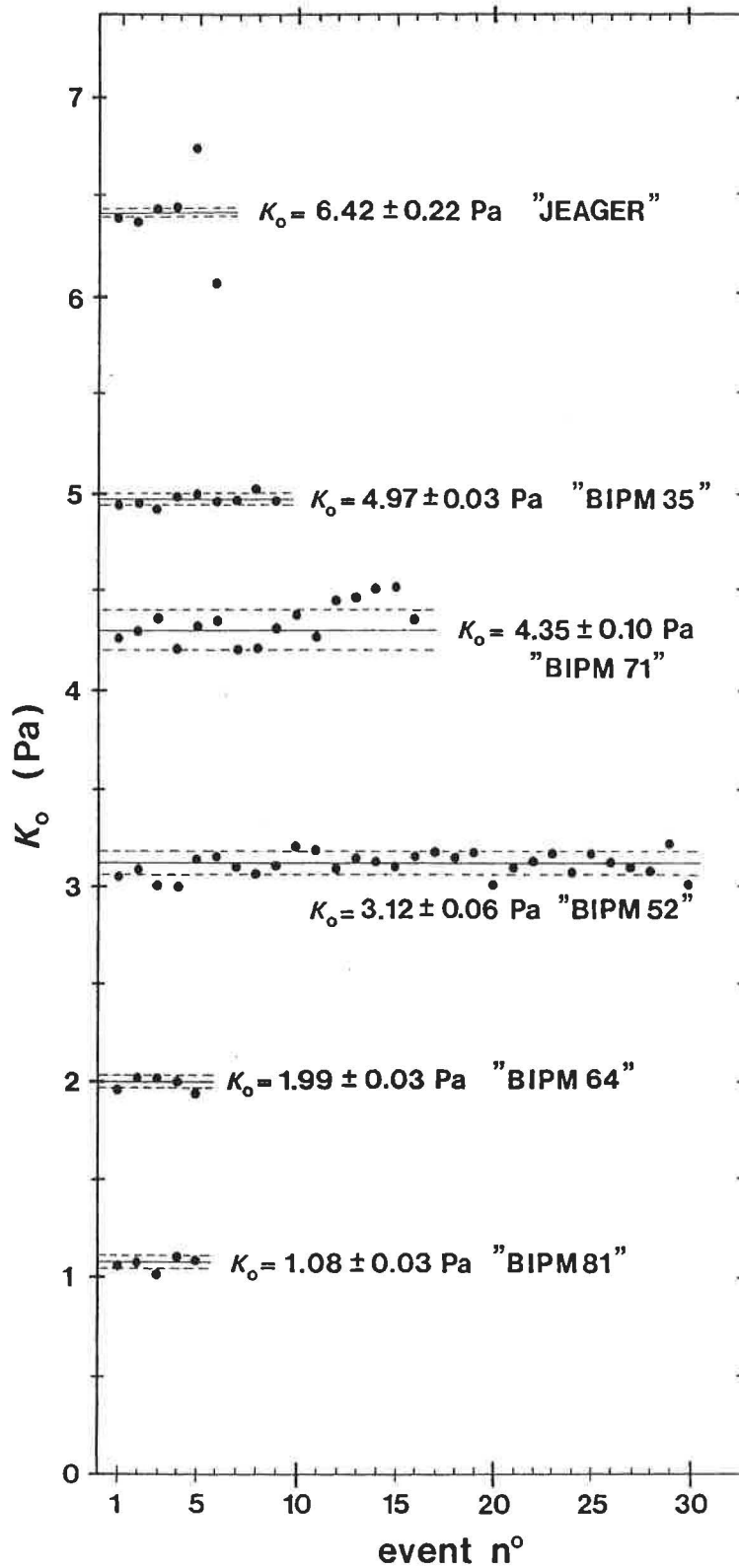


Fig.10-a. Representation of the reproducibility of measurements of six different iodine cells. The mean value of each K_0 and standard deviation are indicated by solid and dashed lines respectively.

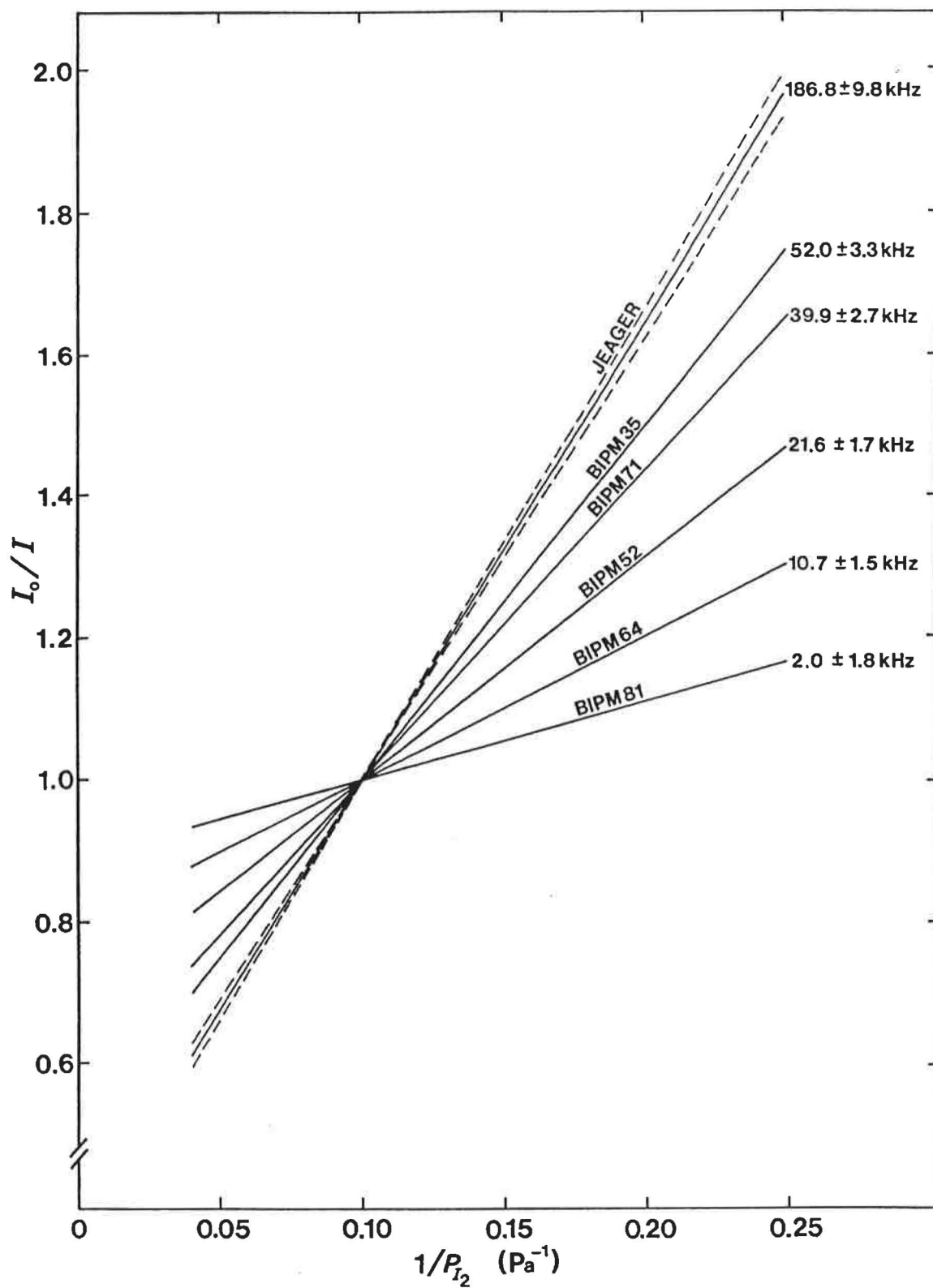


Fig.10-b. Stern-Volmer diagrams for the same six cells as shown in Fig. 10-a. The dashed curves represent the standard deviation. The standard deviations which are within the width of the curve are not marked.

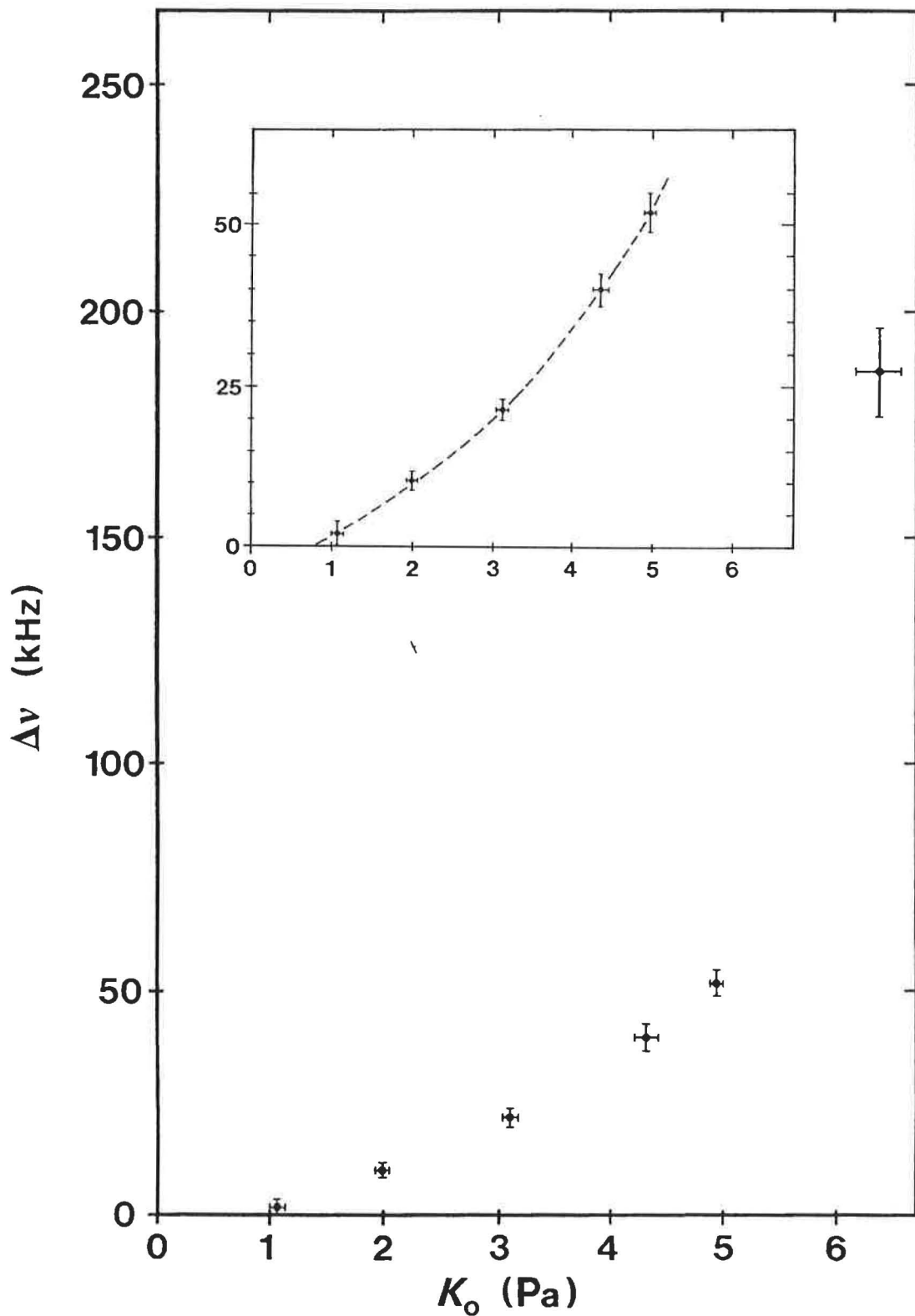


Fig.11. Diagram showing the measured frequency shift $\Delta\nu$ in kHz for an individual cell as a function of K_0 in Pa. The beat frequency measurements were performed at the B.I.P.M. using frequency stabilized intra cavity HeNe lasers at $\lambda=633$ nm.

4.2.2 Cross Sections

Ornstein and Derr [20] have previously used the relationship between the intercept and the slope of the Stern-Volmer curve for a "clean" cell in order to find the self collisional cross section σ_S . One then find the following formula:

$$\frac{L_0}{K_0}(P_x = 0) = \frac{\tau \sigma_S v_I}{kT} \quad (21)$$

They found $\sigma_S = 2.35 \text{ nm}^2$ (which is $\pi \sigma^2$ in their notation) using $\lambda = 501.2 \text{ nm}$ as the exciting wavelength. This value is of the same order as the cross section reported by Paisner and Wallenstein [19] and Capelle and Broida [18] at 501.7 nm. Studying the reciprocal intensity of fluorescence as a function of the foreign gas partial pressure (where the iodine pressure was held constant), the collision cross section for N_2 could further be deduced by Ornstein and Derr [20].

We represent the cross section of the foreign gas by the symbol σ_x . We must not forget however that if several foreign gases are involved, which is most probably the case, we must replace $\sigma_x v_x p_x$ by the sum $\sum \sigma_x v_x p_x$. This implies that a quantitative analysis will be difficult as we do not know which foreign gases are present and to what extent.

As has been pointed out by Capelle and Broida [18], cross sections are difficult to measure. The measurement of self quenching cross sections demands a total absence of foreign gases, but can also be disturbed by wall quenching. Additionally, the accuracy in the pressure determination must be high. This might be the reason for the dispersion in the measured cross sections from various authors which sometimes can be found.

4.2.3 An Attempt at a Quantitative Analysis

A quantitative analysis of the species of the impurities and their abundances using the Stern-Volmer formula is difficult to do for reasons that have been discussed in section 4.2.2. In spite of this, using Eq. (18), we can express the product $\sigma_x p_x v_x$ as

$$\sigma_x p_x v_x = \left(K_0 \left(\sigma_S v_I + \frac{kT}{10\tau} \right) - \frac{kT}{\tau} \right) \frac{1}{(1 - 0.1 K_0)} \quad (22)$$

Let us try to calculate p_x using Eq. (22). Gill and Thompson have previously detected the characteristic emission spectra of CO and N₂ in iodine cells using a weak radio-frequency discharge [14]. They suggest a foreign gas pressure of a few tens of pascals for "bad" cells ($\Delta\nu\approx 200$ kHz). Here we choose N₂ as the only foreign molecule, which means that $v_x=496$ m/s. Ornstein and Derr [20] have measured σ_x for N₂ at $\lambda=501.2$ nm and found $\sigma_x=0.47$ nm². If we now calculate p_x for a good cell ($K_0=1$ Pa) and using $\tau=14$ s [13], $\sigma_S=2.36$ nm² [19], and $v_I=221$ m/s, we obtain $p_x=1$ Pa. Using the same parameters, but taking a bad cell ($K_0=6$ Pa) we get $p_x=32$ Pa. A foreign gas pressure of 1 Pa seems high for a cell that is considered to be almost pure. On the other hand, 32 Pa for a very bad cell does not seem unreasonable, and corresponds well to the pressure predicted by Gill and Thompson [14]. One might ask: are the experimental cross-sections correct, or, does there exist an additional effect that has not been included in our calculations, or, is there that much impurity in an iodine cell?

4.2.4 Impurity Concentration and Frequency Shift Correlation

As we have already experimentally established a relation between $\Delta\nu$ and K_0 , it could be interesting to study the relation between the frequency shift and the contamination. Even if σ_x is not well known, we can propose that the product $\sigma_x p_x v_x$ is.

Fig. 12-a shows the calculated product $\sigma_x p_x v_x$ as a function of K_0 using Eq. (22). Fig. 12-b shows $\Delta\nu$ as a function of the calculated product $\sigma_x p_x v_x$ corresponding to the measured K_0 . This diagram corresponds to the results presented in Fig. 11. We can see that $\Delta\nu$ is very closely proportional to the pressure of foreign gas(es) for cells that are not highly contaminated. This has to our knowledge never been pointed out before.

However, for high contamination rates, $\Delta\nu$ increases rapidly as a function of foreign gas pressure. Gläser [34] has recently studied the frequency shifts as a function of iodine pressure. He found a nonlinear behaviour for small pressures. The non-linear region in Fig. 12-b and the one found by Gläser both correspond to a high concentration region of impurities compared to iodine. Similarly, the linear region of Fig. 12-b and the one found by Gläser correspond to a small concentration of foreign gas compared to iodine. Further investigation of this effect could be interesting in order to arrive at a better understand of the different processes involved.

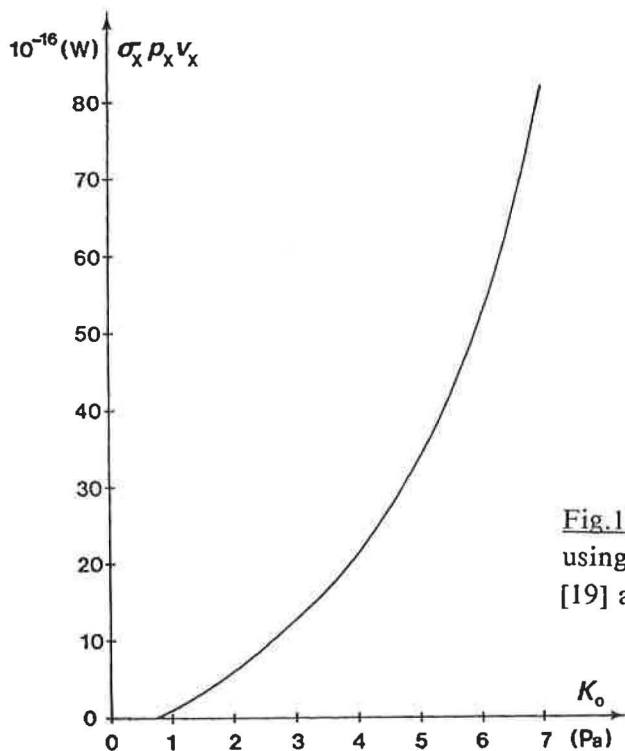


Fig.12-a. $\sigma_x p_x v_x$ (see text) as a function of K_0 using Eq. (22) where $\tau=14 \mu s$ [11], $\sigma_s=2.36 \text{ nm}^2$ [19] and $v_I=156 \text{ m/s}$.

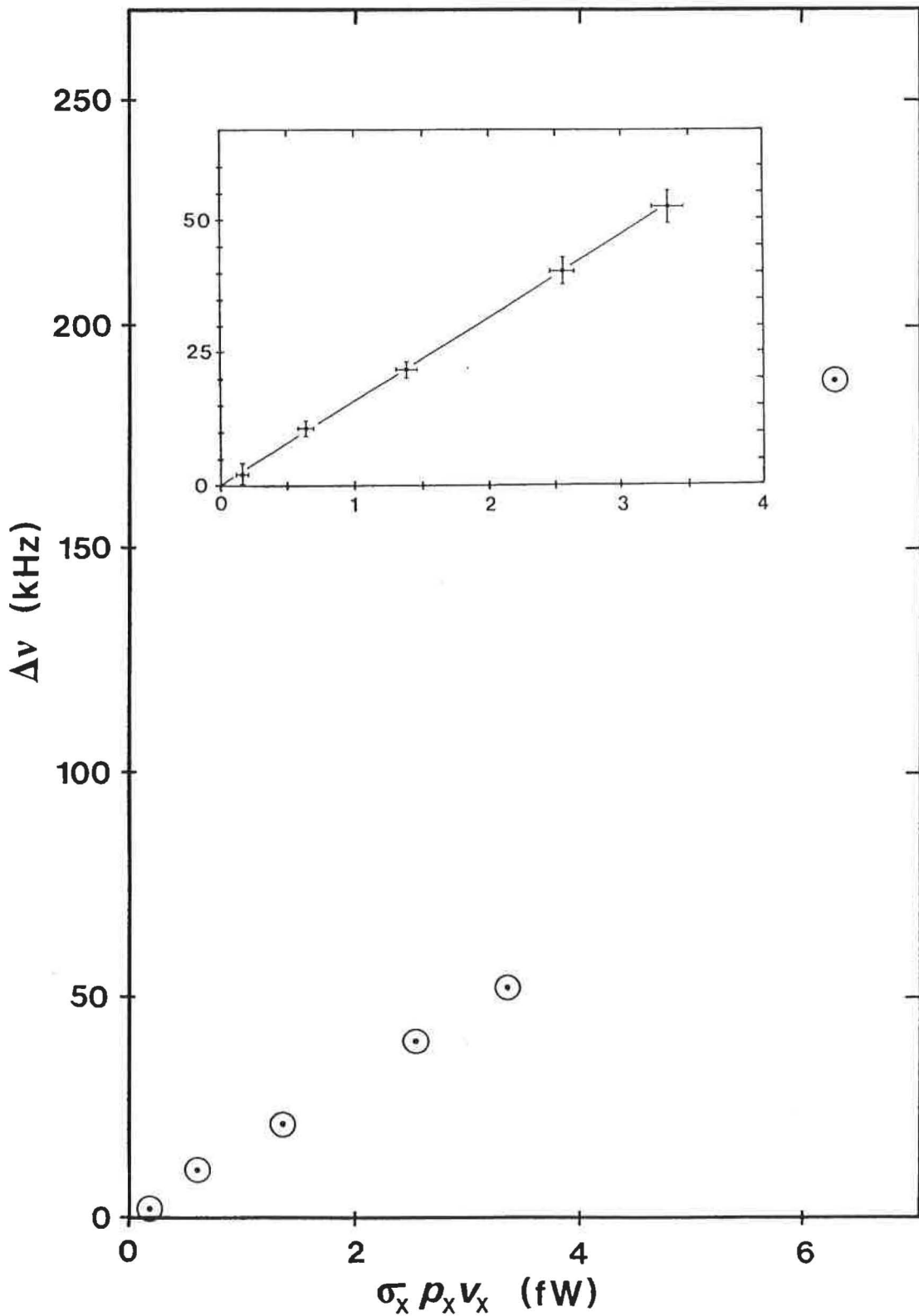


Fig.12-b. Diagram showing the frequency shift $\Delta \nu$ as a function of $\sigma_x \rho_x v_x$ (see text). One can see that $\Delta \nu$ is proportional to ρ_x at low contamination rates. The uncertainty bars correspond to the uncertainty in the measured frequency shift and the uncertainty in σ_s [19] and τ [11] respectively.

4.3 $^{129}\text{I}_2$

Cells filled with $^{129}\text{I}_2$ has with great success been used for frequency stabilization, see for example [35]. Its ro-vibrational spectrum has never been thoroughly investigated as $^{127}\text{I}_2$. However, its spectrum can be calculated by using the accurate molecular constants of $^{127}\text{I}_2$ [29].

Only one cell containing $^{129}\text{I}_2$ was measured to test the Stern-Volmer formula on this molecular isotope. It had been filled at the P.T.B.¹ and showed 3 times less intense fluorescence than any of the cells which had been measured containing $^{127}\text{I}_2$. The slope K_0 for the same cell was 1.43 Pa. The lifetime(s) of the level(s) excited by $\lambda=501.7$ nm is to our knowledge not known. It might be comparable to that of $\lambda=514.5$ nm but this has not been experimentally verified.

4.4 Discussion

4.4.1 Influencing Factors

The reproducibility is worse than the mean uncertainty in K_0 . One possible explanation for this is that any difference in background light belonging to the laser influences the Stern-Volmer slope. It is difficult to eliminate totally the scattered laser light, especially stray light coming from the short cells, like the BIPM52 of 5 cm, where there is a short distance between the cold finger and the windows.

Another factor contributing to the discrepancies may be the uncertainty in the temperature of the iodine cold finger. The temperature calibration was done initially by using an already calibrated thermometer in combination with the electronic display of the servo control. In spite of this, a temperature difference was later found using a thermo couple. This corresponded to a change in K_0 of at most 0.1 Pa. When attaining low temperatures, the radiators of the cooling system have difficulties to dispose the heat produced from the Peltier batteries, and a cold temperature can therefore not be maintained for a long while. This can be solved using water cooling.

When reversing the routine of the measurement, that is, gradually heating the cell from an already low temperature instead of cooling it, a slight hysteresis effect in intensity is sometimes observed. The reason for this is still to be understood.

One should still keep in mind that several lines in fact are excited, where the R(26) 62-0 transition is dominating. Using a monochromator, this the ambiguity could be avoided, but less fluorescence would be obtained.

The factors mentioned in Sec. 2.5 are all contributing to some extent to the observed result. All of them have not been tested by us. However, we checked the effect of radiation trapping by laterally moving the iodine cell in the laser beam in order to change the path length of the fluorescence in the gas. No straight forward change in K_0 was observed.

On the contrary, it was easy to control the influence of Beer's law on the measurements using a 45 cm long iodine cell. detecting fluorescence emanating from a region at 20 cm distance from the beam entrance of the cell, an increase in fluorescence was observed when the pressure was decreased in steps from 25 Pa to 13 Pa, which is the opposite of the expected behaviour. This effect became weaker when the observation region was set closer to the entrance window of the cell. It was found that Beer's law could be neglected observing a region with a light path length of 3 cm or less.

4.4.2 Future Aspects

Gill and Thompson [14] have by spectroscopic means noted that the observed impurities are not the same for two cells showing the same $\Delta\nu$. Furthermore, the observed frequency shifts do not only have to depend on the species and amount of impurities; several other reasons might be responsible, for example the iodine pressure, the curvature of the wavefronts and laser power [34]. The current method can therefore also be a tool to separate some of the factors that influence frequency shifts.

As a prolongation of the experiment described above, it should be interesting to study the vibrational transfer for cells with known frequency shift and Stern-Volmer slope. This could be done in combination with a profundation of spectroscopic investigations of which Gill and Thompson [14] have given an example.

It should also be of interest to perform impurity studies of iodine cells by doing direct lifetime measurements. This could be accomplished by minor modifications of the experimental arrangement discussed above.

Finally, we aim to use the current method for an international inter comparison of iodine cells in a near future, in combination with the saturated absorption beat frequency technique.

5 Conclusion

It is important to know more about impurities in iodine cells and their influence on iodine in order to improve frequency standards using iodine stabilization. The study of laser induced fluorescence as a function of pressure in combination with the use of the Stern-Volmer formula is one of several techniques by which these studies can be accomplished. Six cells filled with $^{127}\text{I}_2$ have been measured and the reproducibility has been studied. The determination of the parameter K_0 , which is related to the impurity concentration, is determined with a relative uncertainty not exceeding $\pm 2\%$. The frequency shift for the same cells has been measured. It was found that the relation between $\Delta\nu$ and $\sigma_x \rho_x v_x$ is linear for small $\Delta\nu$.

The experimental routine is very well suited for a qualitative measurement of impurity concentrations in iodine cells. It is less demanding than this of saturated absorption beat frequency technique, but restricted to measurements of cells with low and moderate impurity concentration, corresponding to frequency shifts less than 60 kHz.

Acknowledgement

I warmly thank members of the BIPM for help concerning various parts of the experimental setup. I am very grateful to Mrs A. Chartier who performed the beat frequency measurements. I am also thankful to Mr J. Sanjaime and all his co-workers who have constructed most mechanics used in the experiment. My appreciation to the Schott society. A special thank to Mr R. Pello for providing radiometric and thermometric utilities, to Mrs D. Le Coz for never failing literature research and to Mr C. Veyradier for the illustrations. Finally I wish to express my gratitude to Mr J.-M. Chartier and Dr L. Robertsson for stimulating discussions and assistance.

6 References

- [1] Documents Concerning the New Definition of the Metre, *Metrologia* 19 (1984) 163.
- [2] M. Broyer, Thèse 3eme Cycle, 1973: Effet Hanle et Résonances en Lumière Modulée de la Molécule I₂.
- [3] W.R.C. Rowley and B.R. Marx, *Metrologia* 17 (1981) 65.
- [4] Ch. J. Bordè, G. Camy, B. Decomps and J. P. Descoubes, *J. Physique* 42 (1981) 1393.
- [5] W. Demtröder, *Laser Spectroscopy: Basic Concepts and Instrumentation*, Chapter 10.2, 2nd corrected edition, Springer Verlag 1982.
- [6] J.M. Chartier, J. Helmcke and A.J. Wallard, *IEEE Trans. Instrum. Meas.* IM-25 (1976) 450.
- [7] F. Spieweck, G. Camy and P. Gill, *Appl. Phys.* 22 (1980) 111.
- [8] Y. Zacharenko, A. Kotkov, N. Melinkov, J.M. Chartier and R. Felder, *Metrologia* 17 (1981) 81.
- [9] F. Bertinotto, P. Cordiale, G.B. Picotto, J.M. Chartier, R. Felder and M.G. Gläser, *IEEE Trans. Instrum. Meas.* IM-32 (1983) 72.
- [10] J.M. Chartier, *IEEE Trans. Instrum. Meas.* IM-32 (1983) 81.
- [11] M. Broyer, J.C. Lehmann and J. Vigué, *J. de Phys.* 36 (1975) 235.
- [12] J.C. Keller, M. Broyer and J.C. Lehmann, *C. R. Acad. Sc. Paris* 277 (1973) B 369.
- [13] M. Broyer, J. Vigué and J.C. Lehmann, *J. Chem. Phys.* 63 (1975) 5428.
- [14] P. Gill and R.C. Thompson, *Metrologia* 23 (1986/87) 161.
- [15] O. Stern and M. Volmer, *Physik. Zeitschr.* 20 (1919) 183.
- [16] F. Spieweck, *IEEE Trans. Instrum. Meas.* IM-34 (1985) 246.
- [17] K.P. Huber and G. Herzberg, *Constants of Diatomic Molecules*, Van Nostrand 1979.
- [18] G.A. Capelle and H.P. Broida, *J. Chem. Phys.* 58 (1973) 4212.
- [19] J.A. Peisner and R. Wallenstein, *J. Chem. Phys.* 61 (1974) 4317.
- [20] M.H. Ornstein and V.E. Derr, *J. Opt. Soc. Am.* 66 (1975) 233.
- [21] K. Sakurai, G. Capelle and H.P. Broida, *J. Chem. Phys.* 54 (1971) 1220.
- [22] A.N. Nesmeyanov, *Vapor Pressure of the Chemical Elements*, Elsevier Publishing Company, 1963.
- [23] L.J. Gillespie and L.A.D. Fraser, *J. Am. Chem. Soc.* 58 (1936) 2260.
- [24] A.B. Lindenberg, *C. R. Acad. Sc. Paris* 273 (1971) C 1017.
- [25] L. Grahm and H. Hertz, *Fysikalisk Mätteknik*, Almqvist och Wiksell, Stockholm 1971.
- [26] J.I. Steinfeld, *J. Chem. Phys.* 44 (1966) 2740.

- [27] R.B. Kurzel, J.I. Steinfield, D.A. Hatzenbuehler and G.E. Leroi, *J. Chem. Phys.* 55 (1971) 4822.
- [28] *Handbook of Lasers with Selected Data on Optical Technology*, CRC Press Inc., Cleveland, Ohio 1971.
- [29] S. Gesternkorn and P. Luc, *Atlas du Spectre d'Absorption de la Molécule d'Iode, 14800-20000 cm⁻¹, complement: Identification des transitions du système (B-X), Assignments of the (B(I₂)-X) Iodine Lines*, Edition C.N.R.S. (1978).
- [30] C. Camy, *Thèse d'état, 1985: Sources Laser Ultrastable en Spectroscopie de Saturation. Réalisation d'Étalons Optiques de Fréquence et Caractérisation de Leurs Qualités*.
- [31] M. Broyer, *Thèse d'état, 1977: Etude de l'Etat B de la Molécule d'Iode par Excitation Laser: Propriétés Magnétiques. Predissociations Gyroscopique et Hyperfine*.
- [32] G. Flory, M. Broyer, J. Vigué et J.C. Lehmann, *Rev. Phys. Appl.* 12 (1977) 901.
- [33] J.M. Chartier and D. Avrons, "Principes Technologiques", *PTB-Bericht, PTB-Me-17* (1977) 13.
- [34] M. Gläser, *Metrologia* 18 (1982) 53.
- [35] J.A. Magyar and N. Brown, *Metrologia* 16 (1980) 63.

July 1989